The Journal of Experimental Biology 208, 2555-2567
Published by The Company of Biologists 2005
doi:10.1242/jeb.01683

Adhesion of echinoderm tube feet to rough surfaces

Romana Santos[1,*], Stanislav Gorb[2], Valérie Jamar[1] and Patrick Flammang[1]

[1]*Académie Universitaire Wallonie-Bruxelles, Université de Mons-Hainaut, Laboratoire de Biologie Marine, 6 Avenue du Champ de Mars, B-7000 Mons, Belgium* and [2]*Max-Planck Institute for Metal Research, Department Arzt, Evolutionary Biomaterials Group, 3 Heisenbergstraße, D-70569 Stuttgart, Germany*

*Author for correspondence (e-mail: romana_santos@yahoo.com)

Accepted 11 May 2005

Summary

Echinoderms attach strongly and temporarily to the substratum by means of specialized organs, the podia or tube feet. The latter consist of a basal extensible cylinder, the stem, which bears an apical flattened disc. The disc repeatedly attaches to and detaches from the substratum through adhesive and de-adhesive secretions. In their activities, echinoderms have to cope with substrata of varying degrees of roughness as well as with changing hydrodynamic conditions, and therefore their tube feet must adapt their attachment strength to these environmental constraints. This study is the first attempt to evaluate the influence of substratum roughness on the temporary adhesion of echinoderm tube feet and to investigate the material properties of their contact surface. It was demonstrated that tube foot discs are very soft (*E*-modulus of 6.0 and 8.1 kPa for sea stars and sea urchins, respectively), have viscoelastic properties and adapt their surface to the substratum profile. They also show increased adhesion on a rough substratum in comparison to its smooth counterpart, which is due mostly to an increase in the geometrical area of contact between the disc and the surface. Tenacity (force per unit area) increases with roughness [e.g. 0.18 and 0.34 MPa on smooth polymethyl-methacrylate (PMMA), 0.21 and 0.47 MPa on rough PMMA for sea stars and sea urchins, respectively] if only the projected surface area of the adhesive footprint is considered. However, if this tenacity is corrected to take into account the actual substratum 3-D profile, surface roughness no longer influences significantly the corrected adhesion strength (e.g. 0.18 and 0.34 MPa on smooth PMMA, 0.19 and 0.42 MPa on rough PMMA for sea stars and sea urchins, respectively). It can be hypothesized that, under slow self-imposed forces, disc material behaves viscously to adapt to substratum roughness while the adhesive fills out only very small surface irregularities (in the nanometer range). It is deposited as a thin film ideal for generation of strong adhesion. Under short pulses of wave-generated forces, attached discs probably behave elastically, distributing the stress along the entire contact area, in order to avoid crack generation and thus precluding disc peeling and tube foot detachment.

Key words: sea star, sea urchin, tube foot disc, tenacity, viscoelastic material, *Paracentrotus lividus*, *Asterias rubens*.

Introduction

Echinoderms have developed attachment mechanisms allowing them to attach strongly and temporarily to the substratum through repeated cycles of attachment/detachment (Flammang et al., 2005). This temporary adhesion relies on specialized organs, the podia or tube feet, which are the external appendages of the water-vascular system (Flammang, 1996). In sea urchins and sea stars, tube feet are specialized for locomotion and anchoring. They consist of a basal extensible cylinder, the stem, which bears an apical flattened disc that makes contact with and adheres to the substratum. The epidermis of the disc contains a duo-gland adhesive system composed of two types of cells: those releasing adhesive secretions and those releasing de-adhesive secretions. Adhesive secretions are delivered through the disc cuticle to the surface of the substratum, where they form a thin film, bonding the tube foot to the substratum (Flammang, 1996). De-adhesive secretions, are released within the cuticle, where they might function as enzymes, causing the discard of its outermost layer, the so-called fuzzy coat (Flammang et al., 1998). Thus, detachment takes place at the level of the fuzzy coat, and the adhesive material is left attached to the substratum as a footprint (Flammang, 1996; Flammang et al., 2005).

During their activities, echinoderms have to cope with substrata of varying degrees of roughness, as well as with changing hydrodynamic conditions, and therefore their tube feet must adapt their attachment strength to these environmental constraints. Although a few studies have evaluated the adhesive capacities of echinoderm tube feet on different substrata (Paine, 1926; Thomas and Hermans, 1985; Flammang and Walker, 1997; Flammang et al., 2005), none

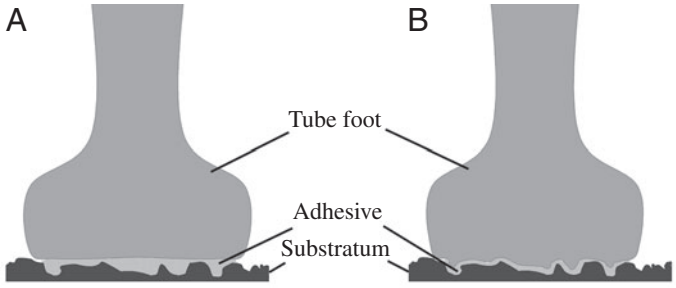

Fig. 1. Diagrammatic representations of the two models proposed for tube foot adhesion to rough surfaces. (A) The tube foot disc remains flat and the adhesive substances are secreted to fill the gaps between surface irregularities or (B) the disc deforms to match the substratum profile and the adhesive is released as an evenly thin film.

of them investigated the influence of substratum roughness. Theoretically, there are two ways by which tube feet can achieve an effective bonding of their discs to a rough surface: either the disc remains flat and more adhesive substances are secreted to fill the gaps between irregularities of the substratum (Fig. 1A) or the disc deforms to match the substratum profile and the adhesive is released as an evenly thin film (Fig. 1B). To address the question of how echinoderms attach to irregular surfaces, we analysed tube foot tenacity (adhesion strength) and disc structural deformation in response to substratum roughness and measured disc mechanical properties in the tube feet of two common European echinoderm species, the sea urchin *Paracentrotus lividus* and the sea star *Asterias rubens.*

Materials and methods

Morphology of tube foot disc

Adult individuals of the echinoid *Paracentrotus lividus* (Lamarck 1816) and the asteroid *Asterias rubens* Linné 1758 were collected intertidally along the Atlantic coast of France (Brest, Brittany) and kept in re-circulating aquariums at 14–15°C and 33‰. Unattached tube feet were dissected from both species, fixed in Bouin's fluid for 24 h and dehydrated in a sequence of graded ethanol.

For scanning electron microscopy (SEM), the tube feet were dried by the critical point method, mounted on aluminium stubs and coated with gold in a sputter coater. They were observed with a JEOL JSM-6100 scanning electron microscope.

For light microscopy (LM), the tube feet were embedded in paraffin wax (Paraplast; Sigma, Steinhem, Germany) using a routine method (Gabe, 1968). They were sectioned longitudinally at a thickness of 7 μm with a Microm HM 340E microtome and the sections were collected on clean glass slides. They were stained with Masson's trichrome or with azocarmine coupled with aniline blue and orange G (Gabe, 1968). The sections were then observed and photographed with a Leitz Orthoplan light microscope equipped with a Leica DC 300F digital camera.

Surface structure and tenacity of tube feet attached to substrata of differing roughness

Two pairs of polymer substrata were used in these experiments, each including one smooth and one textured surface. The first pair of substrata, consisting of polymethyl-methacrylate (PMMA), was manufactured in the laboratory by the use of a two-step moulding technique. The 'rough PMMA' sample was prepared by curing liquid methyl-methacrylate on a negative template shaped on polishing paper with 12 μm particle size. The 'smooth PMMA' sample was obtained in a similar way by using a negative template moulded on a polished surface of polypropylene. The second pair of substrata, made up of polypropylene (PP), was derived from laboratory supplies. The 'smooth PP' samples were prepared by cutting off square pieces (~1 cm^2) from the cover of a micropipette tip rack (MP Biomedicals, Irvine, CA, USA), while the 'rough PP' samples consisted of circular frits (~1 cm in diameter) used in Model 422 Electro-Eluter (Bio-Rad, Hercules, CA, USA).

The surface profile of the different substrata was examined in a scanning white light interferometer (Zygo NewView 5000; Zygo Corporation, Middlefield, CT, USA) at magnifications of 5× and 50×. The device included optics for imaging an object surface and a reference surface together onto a solid-state imaging array, resulting in an interference intensity pattern that was read electronically into a computer. A series of interferograms were generated as the objective was scanned perpendicular to the illuminated surface. They were then individually processed, and finally a complete 3-D image was constructed from the height data and corresponding image plane coordinates. From 3-D images, profilograms of sections and mean surface roughness parameters (mean roughness of the profile, R_a, and maximum height of the profile, R_z) and the profile length ratio (L_r) were obtained.

Tube feet of sea urchins and sea stars were allowed to adhere to clean pieces of the four types of substrata. When a tube foot remained firmly attached to the substratum it was cut off from the animal, fixed and processed for SEM as described above.

Adhesion force measurements of a single tube foot were performed with an electronic dynamometer (AFG 10 N; Mecmesin, Horsham, UK) attached to a Mecmesin-Versa Test motorized stand. This dynamometer measures forces up to 10 N with a precision of 0.002 N. Experiments were performed with sea urchins and sea stars totally immersed in containers filled with seawater. Specimens were put upside-down (to induce tube foot attachment), and a 1 cm^2 piece of substratum, connected to the dynamometer by a surgical thread, was presented to the tube feet. When a single tube foot remained attached to the substratum for at least 10 s, the dynamometer was moved upwards at a constant speed of 15 mm min^{-1} in order to apply a force normal to the disc until it detached, and the maximum adhesive force was recorded (Flammang and Walker, 1997). The piece of substratum was then immediately immersed for 1 min in a 0.05% aqueous solution of the cationic dye Crystal Violet to stain the footprint left by the tube foot after it had become detached (Flammang et al., 1994). This

footprint was measured with a graduated eyepiece mounted on a Leica Laborlux light microscope. It was also photographed, and the digitized image was analyzed with Semaphore® software (Jeol, Tokyo, Japan) to calculate the surface area of the footprint.

The tenacity or adhesive strength (T) was then calculated by dividing the measured adhesion force (F_a) by the corresponding footprint surface area (S):

$$T = F_a/S \quad (1)$$

The tenacity is expressed in N m^{-2} or Pascal (Pa). A corrected tenacity (T_c) was also calculated using the true contact surface area (i.e. taking into account the footprint surface area and the actual substratum profile length):

$$T_c = F_a/(S\,L_r^2) \quad (2)$$

Tenacity measurements were carried out on tube feet from at least three different animals for each species. Results were statistically analysed with Statistica® software (Statsoft Inc., Tulsa, OK, USA) in order to reveal intraspecific differences in tube foot tenacity obtained on substrata of differing roughness. When necessary, logarithmic transformation was used to achieve homoscedasticity, followed by *t*-tests.

Mechanical properties of the tube foot disc

For both sea urchin and sea star tube feet, the mechanical properties of the disc were measured with a micro-force tester (Tetra GmbH, Ilmenau, Germany; see Scherge and Gorb, 2001 for details) composed of three main parts: a platform, a glass spring (with a spring constant of 112 N m^{-1}) and a fibre optical sensor (Fig. 2). The platform held the tube foot clamped by the stem and could be moved up and down by a motorized stage. For each measurement, the platform was moved upwards (loading period) and the tube foot disc brought into contact with a square glass plate attached to the glass spring. Spring deflection was detected by the fibre-optic sensor, whose signal was acquired by a computer. The tube foot disc and the glass surface were kept in contact for 10 s (resting period) and then the platform was moved downward (unloading period) (Fig. 3A). Force *versus* displacement data were continuously recorded by a computer during loading, resting and unloading periods (Fig. 3B). All experiments were carried out at room temperature (22–24°C) and at a relative humidity of 47–56%.

To investigate disc elasticity, the glass plate was brought as close as possible to the tube foot disc. Then, an upward displacement of 100 µm was programmed in order to induce a compression of the disc ranging from 50 to 100 µm. Measurements were performed on 15 randomly chosen tube feet of at least three individuals from each species. As both the disc and the glass spring deform simultaneously, the deflection of the glass spring, when pressed against a hard sample (glass slide), has to be subtracted from the tube foot force–displacement curve to calculate the true deformation of the disc (Fig. 4A). Using this procedure, force–deformation curves were recalculated for the tube feet of both species (Fig. 4B). The loading and unloading parts of the force–deformation curves were then used to obtain a loading

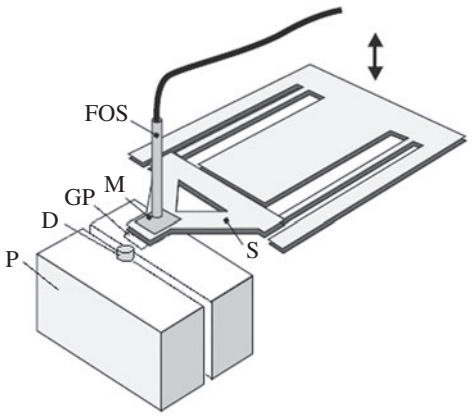

Fig. 2. Micro-force tester used for measurements of the mechanical properties of the tube foot discs. The disc (D) of a cut-off tube foot was mechanically clamped to the platform (P). Driven by a motor, this platform moves the disc towards or away from a smooth glass plate (GP) attached to a glass spring (S). The deflection of the glass spring is monitored by the fibre-optic sensor (FOS) using the monochromatic light sent to and reflected from the mirror (M). The data obtained were transmitted to a computer with a sampling frequency of 25 Hz.

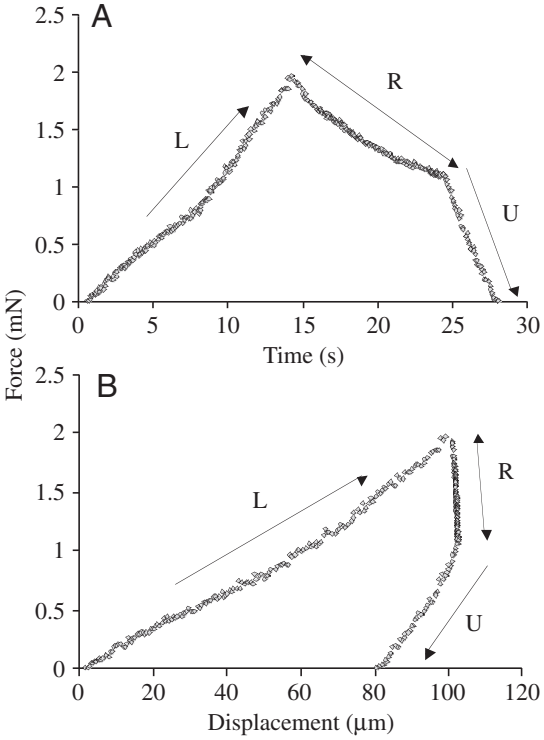

Fig. 3. Typical force–time (A) and force–displacement (B) curves for the disc obtained with the micro-force tester. During the loading process (L), the platform was moved upwards and the disc brought into contact with the glass plate, thus increasing the compression force. Then, the disc and the glass plate were kept in contact for a certain time (resting time, R), during which a rapid decrease in the interacting force (relaxation) is observed. Finally, the platform was moved downwards, unloading the disc (U).

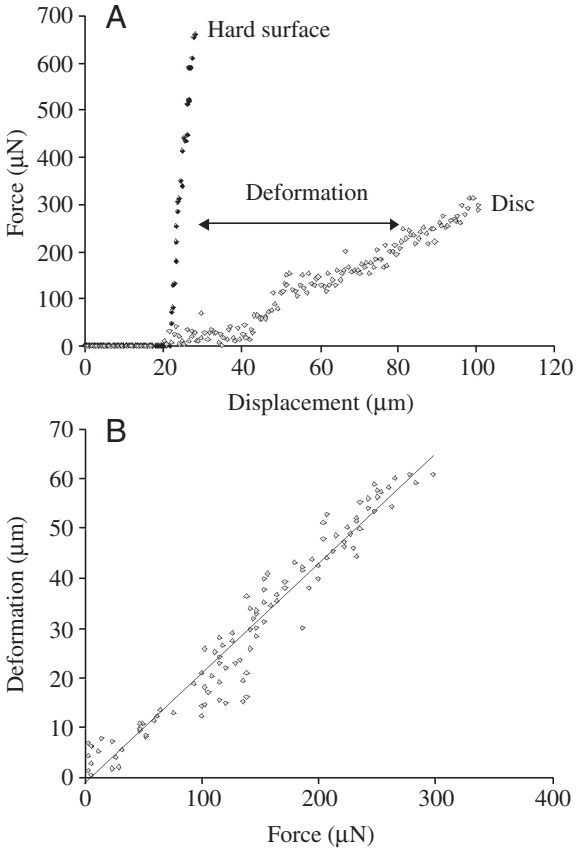

Fig. 4. Force-dependent deformation of the disc. (A) Force–displacement curves during the loading process for the tube foot disc and for a hard sample. (B) Deformation–force curve for the tube foot disc; the solid line represents data linearly fitted with Statistica® software.

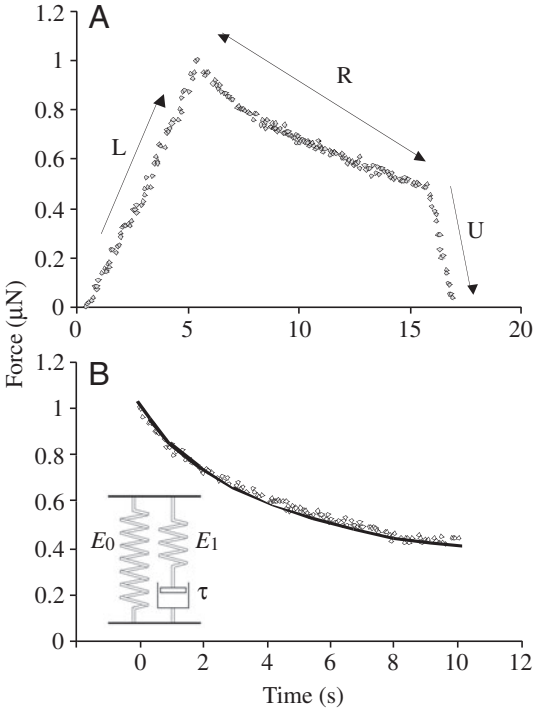

Fig. 5. (A) Typical force–time curve, obtained for the evaluation of the viscous component of the mechanical response of the disc. The curve includes three distinct parts: loading (L), the resting period (R) and unloading (U). Generally, it took 5–7 s to reach a compression force of 1 mN (L) and then the disc was kept in contact with the glass plate for 10 s (R). During the resting period, the force decreased, indicating relaxation of the tissue. (B) Force–time curve of the resting period (R) fitted with a standard linear solid viscoelastic model comprising two elastic moduli (E_0 and E_1), representing two springs connected in parallel, and one time constant (τ), representing a dashpot serially connected to one of the springs (inset).

and an unloading stiffness (expressed in N m^{-1}), corresponding to the slope of the linear part of the curve. The modulus of elasticity (*E*-modulus, expressed in N m^{-2} or Pa) was also calculated as the ratio of stress to strain. Strain is a unitless parameter corresponding to the ratio between disc deformation and disc initial thickness. Stress was obtained by dividing the maximum applied force by the disc cross-sectional area and is expressed in Pa. For calculations, the disc was considered as a cylindrical structure, with a constant geometry of cross-sectional area. Mean values of disc thickness and diameter were obtained using 10 randomly chosen tube feet from at least three individuals of each species.

In each measurement, after loading the disc with a certain compression force, there was a resting period, when the disc and the glass plate were kept in contact without further loading or unloading (Fig. 3). At the beginning of the resting period, the measured force exponentially decreased. The force decrease is due to the relaxation of the tube foot disc material. This behaviour indicates viscoelastic properties of the disc material. To study the viscous component of the disc material properties in detail, we designed a new experiment, in which the disc was deformed by the glass plate up to a pre-defined normal force of 1 mN. This procedure was repeated with four tube feet of each species and data plotted as force–time curves (Fig. 5A). Then, the relaxation part (resting period) of the force–time curve was fitted with a standard linear solid model (Wainwright et al., 1976; Vincent, 1990) in which the zero point of time corresponds to the maximal load prior to relaxation (Fig. 5B). This model includes two elastic moduli (E_0 and E_1), representing two springs connected in parallel, and one time constant (τ), representing a dashpot serially connected to one of the springs. The formula used for fitting was:

$$F_c = \pi r^2 (\Delta l/l) (E_0 + E_1 e^{t/\tau}) \quad (3)$$

where F_c is the compression force (μN), r is the radius of the disc (μm), Δl is deformation (μm), l is the thickness of the disc (μm) and t is time (s).

The micro-force tester used could not operate in seawater, thus all the experiments had to be performed in air. The tube feet tested were initially moist but became dry after a certain time. To minimize desiccation of the disc material, the dissected tube feet were taken out of seawater just before mechanical tests. To test the influence of evaporation, the time of each measurement was recorded. Measurements on every

single disc were repeated at every minute of desiccation of the disc for 5 min. Fluctuations in disc thickness and diameter were also measured at every minute of desiccation up to 5 min.

Data were analysed with Statistica® software to search for differences in the mechanical properties of the tube feet between the two species studied, as well as for a possible effect of evaporation. When necessary, data were log-transformed followed by multi-factorial analysis of variance (ANOVA) and Tukey tests for multiple comparisons. The variability explained by each factor is derived from the sum of squares.

Results

Morphology of tube foot disc

In both the sea urchin *Paracentrotus lividus* and the sea star *Asterias rubens*, the tube feet consist of a basal extensible cylinder, the stem, and an enlarged and flattened apical extremity, the disc (Fig. 6A,B). The tube feet of *P. lividus* bear discs (895±106 μm in diameter, mean ± S.D.) larger than their stems (~300 μm in diameter), the latter being able to actively extend up to 15 mm. On its distal surface, the disc bears a circular groove that clearly separates a large central area from a narrow peripheral area (Fig. 6A). Clusters of 4–5 μm-long cilia cover the peripheral area of the disc, whereas the central area has shorter 1 μm-long cilia (Fig. 6C). On average, tube feet of *A. rubens* have discs of 1300±123 μm (mean ± S.D.) in diameter; their stems have roughly the same diameter as the discs and can reach 20 mm in length, when protracted. The rim and the centre of the disc are not clearly demarcated and the whole surface is regularly covered by cilia 1 μm long and pores

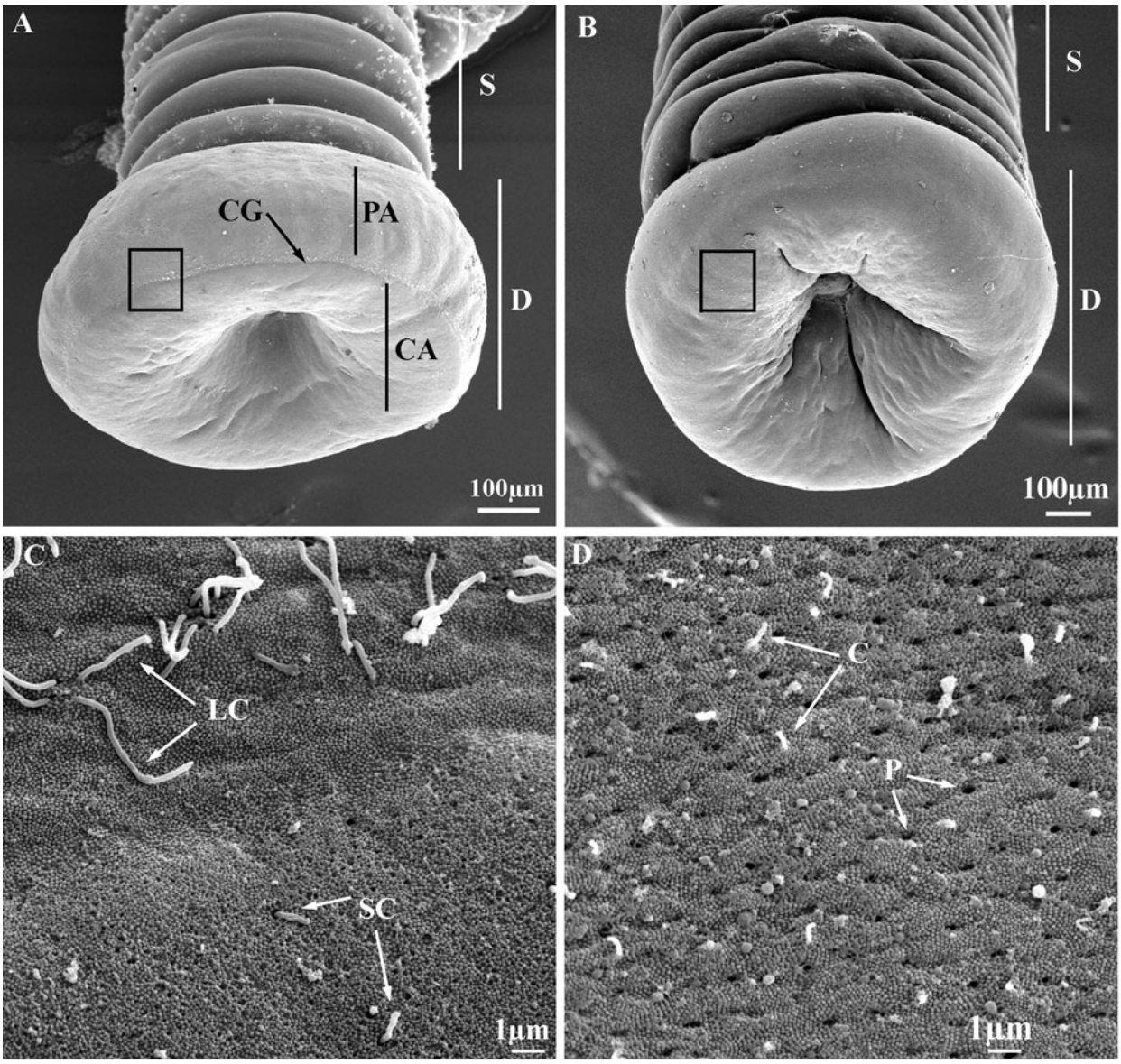

Fig. 6. External morphology of non-attached tube feet of *Paracentrotus lividus* (A,C) and *Asterias rubens* (B,D). Abbreviations: C, cilia; CA, central area; CG, circular groove; D, disc; LC, long cilia; P, pore; PA, peripheral area; S, stem; SC, short cilia. Boxed areas in A and B are magnified in C and D.

400 nm in diameter (Fig. 6D). A typical central depression is visible on unattached tube feet of both species (Fig. 6A,B).

Discs of both species consist of two layers of approximately equal thickness: a deeper supporting structure and a distal pad making contact with the substratum (Fig. 7A,B). The supporting structure consists mostly of a circular plate of connective tissue, the so-called terminal plate, that is continuous on its proximal side with the connective tissue sheath of the stem. The centre of the terminal plate or diaphragm is very much thinner than its margin and caps the ambulacral lumen. In *P. lividus*, the terminal plate (supporting structure) encloses a calcified skeleton made up of four large ossicles arranged in a circle around the ambulacral lumen. In *A. rubens*, on the other hand, the terminal plate is composed of densely packed collagen fibres. In both species, the pad is composed of a thick adhesive epidermis reinforced by bundles of collagen fibres. Numerous branching connective tissue septa emerge from the distal surface of the terminal plate and manoeuvre themselves between the epidermal cells. The thinnest, distal branches of these septa attach apically to the support cells of the epidermis. In *P. lividus*, these septa form an irregular meshwork, whereas in *A. rubens* they are arranged as well-defined radial lamellae [Fig. 7C,D; for a more detailed description of the disc epidermis of sea stars and sea urchins tube feet, see Flammang et al. (1994) and Flammang and Jangoux (1993)].

Surface structure and tenacity of tube feet attached to substrata of different roughness

Table 1 shows the profile parameters (R_a, R_z and L_r) for the tested substratum surfaces. The two smooth substrata did not present any important protuberance on their surfaces (Figs 8A,B,E,F, 9A). The profile parameters of both smooth substrata (PMMA and PP) were clearly lower than those of their rough equivalents (Table 1). The surface profile parameters measured for the smooth PMMA samples were very similar to those from the smooth PP samples (Table 1). On the other hand, the mean roughness (R_a) and maximum height (R_z) of the rough PP samples were 7–16 times larger in comparison with the rough PMMA samples (Table 1). Indeed,

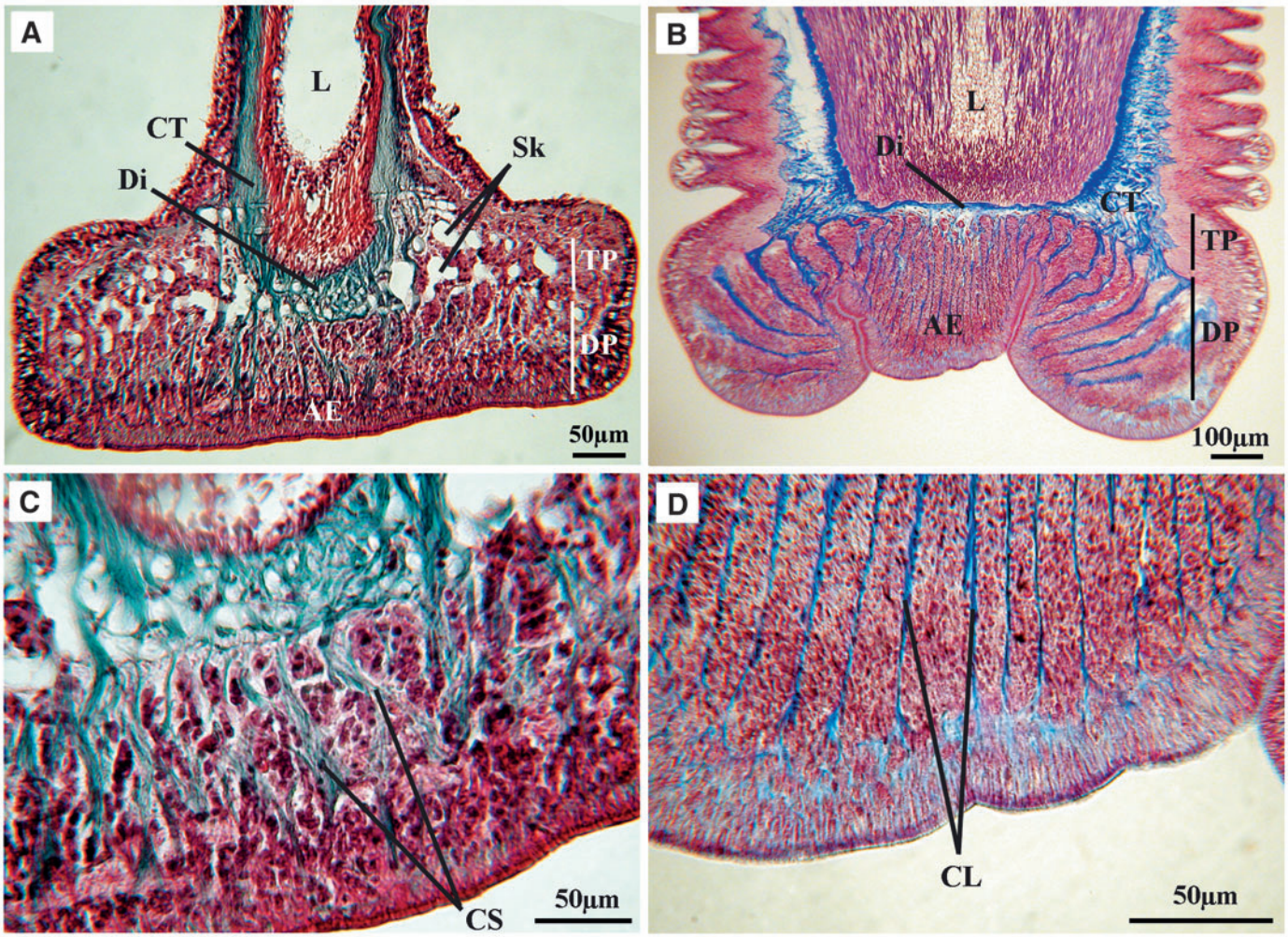

Fig. 7. Longitudinal sections through the discs of the tube feet of *Paracentrotus lividus* (A,C) and *Asterias rubens* (B,D; the section goes through the margin of the disc to show the connective tissue radial lamellae). Abbreviations: AE, adhesive epidermis; CL, connective tissue radial lamellae; CS, connective tissue septa; CT, connective tissue layer; Di, diaphragm; DP, distal pad; L, lumen; Sk, skeleton; TP, terminal plate.

Table 1. *Mean values (±S.D.) of surface profile parameters obtained from 3-D images* (N=*3) of the four types of substrata*

	PMMA		PP	
Profile parameters	Smooth	Rough	Smooth	Rough
Low magnification (5×)				
R_a (μm)	0.36±0.13	1.74±0.65	0.20±0.03	27.02±1.21
R_z (μm)	10.52±0.57	16.22±2.80	16.87±18.65	262.14±50.32
High magnification (50×)				
R_a (μm)	0.07±0.01	1.98±0.27	0.03±0.01	18.73±11.77
R_z (μm)	1.51±0.09	15.19±2.29	3.37±3.35	106.65±29.83
L_r	1.004±0.001	1.055±0.011	1.008±0.001	1.776±0.286

R_a, mean roughness of the profile; R_z, maximum height of the profile; L_r, profile length ratio.

the surface of the rough PMMA substratum was regularly micro-textured (Figs 8C,D, 9D) whereas the surface of the rough PP substratum was very irregular, being made of aggregated particles (Figs 8G,H, 9G). Furthermore, for both PMMA and PP, the profile length ratio (L_r) was higher on rough than on smooth substrata (Table 1). The larger the value of L_r, the sharper or crisper the surface profile appears and the larger the true surface area of the substratum is.

The surface topography of tube foot discs attached to the various substrata was investigated by SEM. In the two species, the discs attached to smooth substrata presented flat and relatively smooth surfaces, whereas those attached to rough substrata had irregular surfaces (Fig. 9). Discs attached to rough PMMA were covered with evenly spaced slight indentations (Fig. 9E,F) whereas discs attached to rough PP showed larger and deeper indentations (Fig. 9H,I). The tube foot discs of *P. lividus* and *A. rubens* therefore seem to replicate the substratum profile (Fig. 9), although there is an important variability from one tube foot to another. This variability may be explained by the fact that no external pressure was applied on the tube feet. Therefore, the force with which the disc was pressed on the substratum was only due to their own natural movements and was probably quite variable.

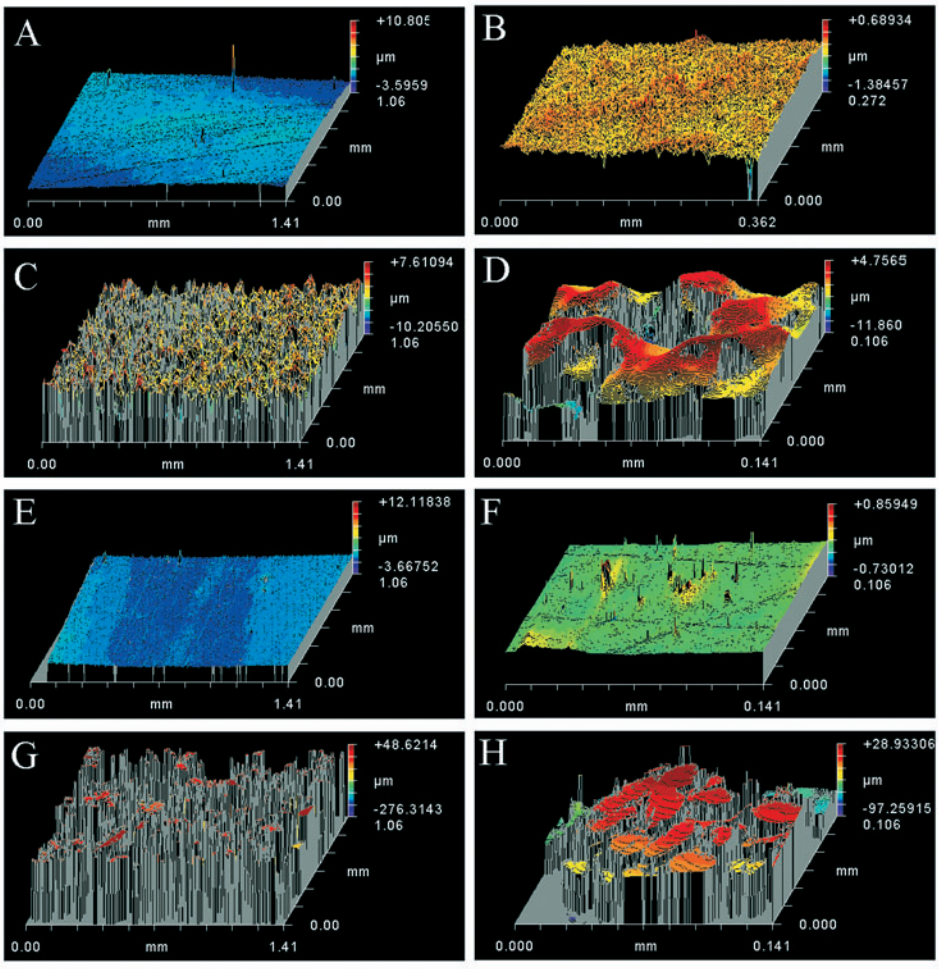

Fig. 8. 3-D images of the surface of the different substrata at low (5×, left column) and high (50×, right column) magnification. (A,B) Smooth polymethyl-methacrylate (PMMA); (C,D) rough PMMA; (E,F) smooth polypropylene (PP); (G,H) rough PP.

Fig. 10 summarizes the results of adhesion measurements from the tube foot discs of the two species considered, when attached to substrata of different roughness. In sea urchins, mean tenacity was significantly influenced by the roughness of the substrata. On both PMMA and PP substrata, the tube feet of *P. lividus* produced higher tenacity on the rough substrata than on the smooth ones (0.34 and 0.47 MPa for PMMA; 0.14 and 0.28 MPa for PP; *t*-test, $P<0.04$). In sea stars, tube foot tenacity was also higher on the rough PMMA

substratum than on its smooth counterpart (0.18 and 0.21 Mpa, respectively) but this difference was not significant (*t*-test, P=0.17). There are no tenacity data on PP because the tube feet of *A. rubens* did not adhere firmly enough to this substratum. In terms of corrected tenacity, however, roughness no longer influenced tube foot adhesion significantly (*P. lividus* – 0.34 and 0.42 MPa for PMMA, 0.14 and 0.09 MPa for PP; *A. rubens* – 0.18 and 0.19 MPa for PMMA; *t*-test, P>0.14). Between species, sea urchin tube feet produced significantly higher tenacities (T and T_c) than sea star tube feet on both smooth and rough PMMA substrata (*t*-test, P<0.003).

Mechanical properties of the tube foot disc

In both species, there was a gradual deformation of tube foot disc under the applied force during the loading process (Fig. 4B). In freshly cut-off tube feet, the mean deformation of the disc was 68.1±11.1 μm (mean ± S.D.) in *P. lividus* and 77.8±11.5 μm in *A. rubens*, corresponding to a compression

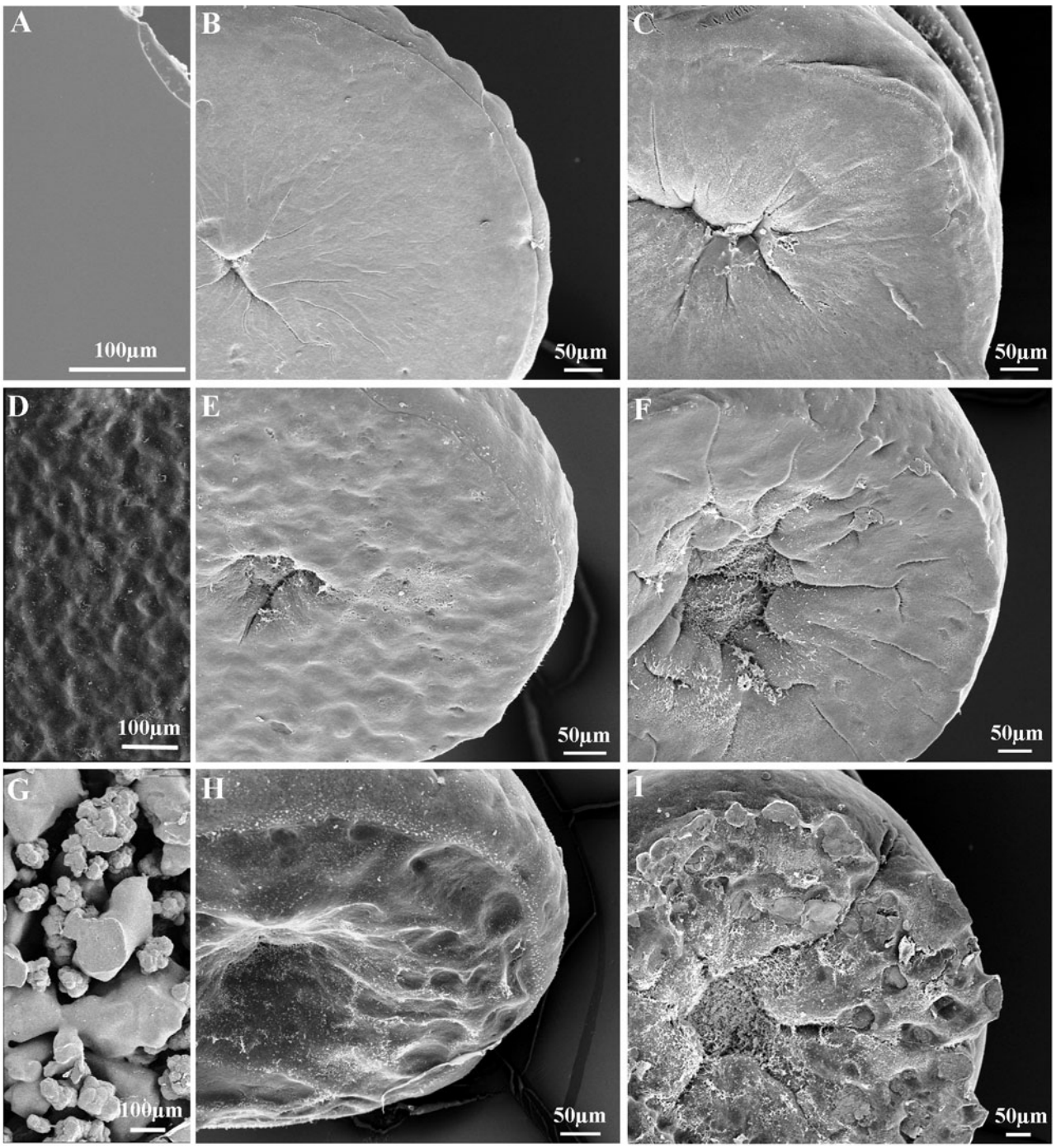

Fig. 9. SEM images of the surface of smooth PMMA (A), rough PMMA (D) and rough PP (G) samples and of the distal surfaces of discs attached to each of these substrata (B,C; E,F and H,I; respectively). (B,E,H) *Paracentrotus lividus*; (C,F,I) *Asterias rubens*.

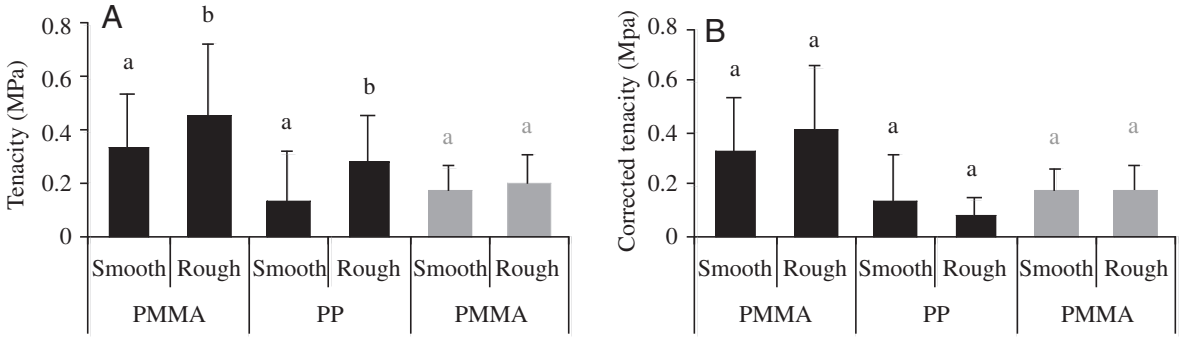

Fig. 10. Mean tenacity (A) and corrected tenacity (B) (± S.D., *N*=30) of the tube feet of the sea urchin *Paracentrotus lividus* (black bars) and the sea star *Asterias rubens* (grey bars), using a separation speed of 15 mm min^{-1}. Significant intraspecific differences between means for each type of substrata are indicated by letters in superscripts; means sharing the same letter are not significantly different ($P \geqslant 0.05$, *t*-test).

force of 1.5±1.2 mN and 1.2±1.1 mN, respectively. Since the mean thickness of the disc was 224±34 μm for sea urchins and 455±32 μm for sea stars, their deformations were approximately 30 and 17%, respectively. Table 2 summarizes the results for disc stiffness and elastic modulus measured each minute for 5 min on discs from both species. Two-way ANOVA (species and evaporation time as independent variables) revealed that loading and unloading stiffness as well as elastic modulus of discs vary significantly between species (Table 4). The three variables were always higher in *P. lividus* than in *A. rubens*, indicating that sea urchins have stiffer discs than those of sea star. An additional two-way ANOVA (part of the curve and evaporation time as independent variables) showed that, in both species, stiffness did not vary significantly during loading and unloading of the discs at any time of evaporation ($P>0.05$). In *P. lividus*, a significant variability of the elastic modulus with time of evaporation was observed (Tables 2, 4). However, no consistent relationship was found between disc elasticity and time of desiccation, at least up to 5 min.

Table 3 presents the mean values of the three parameters of the standard linear solid viscoelastic model applied to measurements of the tube feet from both species. In order to search for differences between the species studied as well as the times of evaporation, a two-way ANOVA was performed for the three parameters of the model (Table 4). The elastic modulus E_0 did not differ either between the two species or between the different times of evaporation. The elastic modulus E_1 was slightly higher in *P. lividus* than in *A. rubens*, but no effects were observed in terms of disc desiccation. The time of relaxation (τ) did not differ between the two species but was significantly affected by the time of evaporation. Further analysis within each species showed that, in *A. rubens*, the elastic modulus E_0 was significantly higher at 4 min of evaporation than at 1 min and the time of relaxation was significantly higher at 2 min of evaporation than at 0 min (Table 3). However, the differences observed are very variable and no consistent pattern could be found.

Discussion

Many marine benthic organisms are equipped with adhesive organs, the secretions of which allow them to attach to the substratum. Adhesion may be permanent, as in sessile

Table 2. *Mean values (±S.D.) of loading and unloading stiffness and* E*-modulus measured on the tube foot disc of the two species studied*

	Evaporation time (min)					
	0	1	2	3	4	5
Asterias rubens						
Number of tube feet tested	15	8	8	6	7	8
Loading stiffness (N m^{-1})	17.41±17.94^{a}	9.40±8.76^{a}	7.41±4.92^{a}	13.02±9.51^{a}	11.05±11.49^{a}	28.92±40.79^{a}
Unloading stiffness (N m^{-1})	29.28±47.95^{a}	12.49±13.68^{a}	16.32±13.86^{a}	18.15±15.88^{a}	13.74±8.24^{a}	28.37±25.84^{a}
E-modulus (kPa)	6.03±6.22^{a}	3.62±3.30^{a}	3.09±1.97^{a}	5.95±4.35^{a}	5.68±5.08^{a}	8.36±10.46^{a}
Paracentrotus lividus						
Number of tube feet tested	15	10	12	12	11	8
Loading stiffness (N m^{-1})	27.30±24.45^{a}	21.76±26.68^{a}	28.08±37.07^{a}	82.09±130.17^{a}	176.89±240.61^{b}	72.66±67.02^{a}
Unloading stiffness (N m^{-1})	32.90±34.44^{a}	43.22±70.76^{a}	83.41±165.69^{a}	72.79±72.80^{a}	58.68±82.67^{a}	111.52±107.84^{a}
E-modulus (kPa)	8.05±7.12^{a}	7.96±8.14^{a}	11.82±17.73^{a}	27.62±40.81^{a,b}	70.02±182.24^{b}	51.04±46.09^{a,b}

Significant intraspecific differences between means are indicated by letters in superscripts; means sharing at least one letter are not significantly different ($P \geqslant 0.05$, Tukey test for multiple comparison).

Table 3. *Mean values (±S.D.) of parameters of the standard linear solid viscoelastic model applied to measurements on the tube foot disc of the two species studied*

	Evaporation time (min)					
	0	1	2	3	4	5
Asterias rubens						
Number of tube feet tested	4	4	4	3	2	4
E_0 (kPa)	2.03±0.62[a]	3.20±0.95[a,b]	4.45±1.76[a,b]	5.77±1.31[a,b]	9.06±5.41[b]	3.93±2.65[a,b]
E_1 (kPa)	3.40±1.67[a]	1.86±0.31[a]	3.27±3.19[a]	3.06±1.64[a]	5.04±2.86[a]	5.67±5.40[a]
τ (s)	7.50±2.48[a]	3.11±0.51[b]	4.08±1.44[a,b]	5.27±0.58[a,b]	7.22±0.08[a,b]	5.74±1.98[a,b]
Paracentrotus lividus						
Number of tube feet tested	4	4	2	4	2	2
E_0 (kPa)	4.14±2.22[a]	7.42±5.30[a]	11.96±1.53[a]	7.73±12.01[a]	1.71±0.73[a]	5.09±4.59[a]
E_1 (kPa)	5.41±2.08[a]	4.25±1.54[a]	5.39±1.28[a]	3.57±2.16[a]	3.61±0.99[a]	8.31±6.99[a]
τ (s)	5.11±1.75[a]	4.48±1.41[a]	2.77±0.45[a]	4.10±0.62[a]	5.40±0.40[a]	5.04±0.66[a]

Significant intraspecific differences between means are indicated by letters in superscripts; means sharing at least one letter are not significantly different ($P \geqslant 0.05$, Tukey test for multiple comparison).

invertebrates that cement themselves to the substratum (e.g. barnacles), or non-permanent, as in those benthic organisms that move around at some times and attach themselves strongly but temporarily to the substratum at other times (e.g. limpets or echinoderms) (Walker, 1987; Whittington and Cribb, 2001; Flammang et al., 2005). The evaluation of the adhesive strength in marine invertebrates is usually done by measuring their tenacity, which is the adhesion force per unit area and is expressed in Pa. According to the taxonomic group considered, tenacities of marine organisms range from ~1 to 2000 kPa (reviewed by Walker, 1987). However, many studies have shown that several factors may profoundly influence the tenacity of invertebrates (see, for example, Grenon and Walker, 1981). For example, the chemical characteristics (e.g. hydrophobicity, surface charges) of the substratum are known to change the tenacity of organisms by up to an order of magnitude (Young and Crisp, 1982; Yule and Walker, 1987). In general, the tenacity of attached organisms, whether permanently or non-permanently attached, is proportional to the polarity (usually estimated by water-based contact angle) of the substratum (see, for example, Grenon and Walker, 1981; Flammang and Walker, 1997; Waite, 2002); i.e. they adhere much more strongly to polar than to non-polar substrata. This can be explained by the fact that marine bioadhesives are rich in charged and polar residues (Flammang, 2003), which are probably involved in adhesive interactions with polar substrata through hydrogen and ionic bonding (Waite, 1987). It is also generally admitted that marine invertebrates adhere more strongly to rough surfaces than to smooth ones (Walker, 1987). However, in many studies, when substrata of differing roughness were used, they were also of differing chemical composition, rendering comparisons non-valid. In fact, very few studies have really investigated the influence of substratum roughness on adhesion of marine invertebrates, and the present study is the first attempt to evaluate this influence on the temporary adhesion of echinoderm tube feet.

Attachment strength of tube feet on rough substrata

Adhesion of echinoderm tube feet appears to be stronger on rough substrata than on smooth ones. The tube foot discs of *Paracentrotus lividus* showed a significantly higher tenacity on rough substrata in comparison with smooth substrata. The increase in tenacity was of approximately 26% on PMMA and 50% on PP. Tenacity values obtained for discs of *Asterias rubens* attached to smooth and rough PMMA also showed an increase but, contrary to the data obtained for echinoids, this increase was not significant. As for corrected tenacity, it never varied significantly with substratum roughness. The values of tenacity measured on the two polymer substrata were in the same range as those reported in previous studies for single tube

Table 4. *Variability (%) in the mechanical properties of echinoid and asteroid tube foot disc explained by the two factors considered (species and time of evaporation)*

	Loading–unloading experiment			Stress–relaxation experiment		
	Loading stiffness	Unloading stiffness	*E*-modulus	E_0	E_1	τ
Species	15.43	6.97	14.17	0.11*	10.68	5.05*
Time of evaporation	7.51*	5.01*	9.85	14.64*	13.51*	39.70
Species × time of evaporation	4.33*	2.76*	3.93*	26.98*	8.23*	13.21*
Residual	72.73	85.26	72.05	58.27	67.57	42.03

Asterisk indicates non-significant percentages ($P \geqslant 0.05$, two-way ANOVA).

feet of *A. rubens* (0.2 MPa; Flammang and Walker, 1997) and *P. lividus* (0.29 MPa; Flammang et al., 2005) attached to smooth glass slides.

Influence of surface roughness on adhesion has only been investigated in two other marine invertebrate taxa: barnacles and limpets. Barnacles attach permanently to the substratum as adults but have a larval stage, the cyprid, that uses temporary adhesion (Yule and Walker, 1987). The cyprid larva of barnacles adheres temporarily to the substratum by antennulary attachment discs while it explores a surface during settlement. These discs demonstrate high deformability, allowing them adaptation to the substratum profile, and produce an adhesive secretion. Surface roughness influences the force required to detach the cyprids. An increase in the roughness of a PMMA substratum from 0.03 to 1.0 μm (R_a) results in an increase of antennule tenacity from 0.08 and 0.14 MPa (Yule and Walker, 1984, 1987). At metamorphosis, the cyprid secretes a cement to attach itself permanently to the substratum. A roughened surface also affords the newly metamorphosed barnacle better adhesion than does a smooth surface; increasing the roughness of the PMMA from 0.03 to 1 μm significantly increases the tenacity from 0.16 to 0.5 MPa (Yule and Walker, 1987). In limpets, the effect of different substrata on tenacity was investigated in emersed animals attached to smooth glass, smooth and rough slate and smooth PMMA (Grenon and Walker, 1981). The highest tenacity values where obtained on glass and rough slate (0.23 MPa), followed by smooth slate and PMMA (0.19 and 0.17 MPa, respectively).

In sessile invertebrates attaching permanently to the substratum, the high tenacity measured on rough surfaces is most likely due to mechanical interlocking (Yule and Walker, 1987). The cement secreted by these organisms is initially fluid and able to infiltrate deeply the pores and crevices of the substratum. After polymerization, the cement becomes a material with high cohesive strength, interlocking with the substratum (Cheung et al., 1977; Yule and Walker, 1987). This is corroborated by observations made on the cement of barnacles (Dougherty, 1990), tubeworms (Roscoe and Walker, 1995) or mussels (Crisp et al., 1985), which forms a perfect cast of the surface features of the substratum after the animal had been carefully detached. For invertebrates using non-permanent adhesion, on the other hand, mechanical interaction between the adhesive and the substratum surface is presumably not involved in the increase of adhesive strength observed on rough substrata compared with smooth ones. Several other explanations, which are not mutually exclusive, have been proposed for this effect. Grenon and Walker (1981) suggested that, as surface roughening alters the contact angle between water and the substratum (Baier et al., 1968), it would presumably also modify the spreading of the adhesive secretion and consequently the tenacity observed for certain organisms. However, according to Kendall (2001), roughening does not modify the contact angle of water but rather retards the formation of this wetting angle on surfaces (hysteresis effect). This may therefore modify the speed of adhesion but not the strength of adhesion. Friction could also explain the more important force required to detach organisms from rough surfaces because the irregular surface introduces shear forces within the adhesive layer even when normal pulls are applied, as in the present study and in those on barnacle cyprids and limpets. A third explanation is the retardation of crack propagation. Cracking is the mechanism by which an adhesive material detaches from a surface (Kendall, 2001). On a rough surface, crack propagation would have to follow a much longer, nonrectilinear path at the interface (Baier et al., 1968), resulting in an increased adhesive strength. A final explanation is the increase in geometrical area of contact as a result of roughening, which leads to a more important adhesive force but not a higher tenacity (both force and surface area increase together). However, as substratum roughness is usually not taken into account, the contact area is underestimated from the surface area of the adhesive organ (e.g. the surface area of the foot in limpets; Grenon and Walker, 1981), hence the higher apparent tenacity on rough substrata.

In our study, a corrected tenacity was calculated, which includes the actual profile length of the substratum and therefore the true surface area of contact. The fact that this corrected tenacity did not vary significantly with substratum roughness pleads in favour of the last hypothesis (i.e. adhesion force increase due to the increase in geometrical area of contact on rough surfaces). This corrected tenacity assumes that detachment occurs at the interface between the substratum and the adhesive. However, in the case of echinoderms, detachment generally occurs at the interface between the tube foot disc and the adhesive, which is left as a footprint on the substratum. Therefore, on irregular surfaces, the corrected tenacity is valid only if the tube foot disc deforms to match the substratum profile. Such a deformation was demonstrated by the SEM pictures taken on the disc surface of the tube feet attached to the rough polymers. It is possible due to the material properties of the disc.

Viscoelastic properties of the tube foot disc

Measurement of the mechanical properties of the tube foot disc in *P. lividus* and *A. rubens* demonstrated that this structure is made up of a very soft material with a mean elastic modulus ranging from 3 to 140 kPa. Loading and unloading stiffness, as well as the elastic modulus of the disc, was higher in sea urchins than in sea stars (Table 2). Higher stiffness of sea urchin discs might be a consequence of the presence of a calcified skeleton within their connective tissue. Furthermore, no significant differences were found between loading and unloading stiffness and no consistent desiccation effect could be established. Regarding the stress–relaxation experiments, a standard linear solid viscoelastic model was used to describe disc behaviour during the contact with the substratum. This model comprises two elastic moduli (E_0 and E_1), representing two springs (simulating the elastic behaviour of solids whose resistance to deformation is a function of applied force), and one time constant (τ), representing a dashpot (simulating the viscous behaviour of fluids whose resistance to deformation

depends on the rate at which they are deformed). The elastic modulus E_0 (4.1 kPa for sea urchins and 2.0 kPa for sea stars at 0 min) and the time of relaxation τ (5.1 s for sea urchins and 7.5 s for sea stars at 0 min) did not differ between the two species whereas the elastic modulus E_1 was slightly higher (P=0.049) in *P. lividus* (5.4 kPa at 0 min) than in *A. rubens* (3.4 kPa at 0 min). None of these variables were consistently influenced by the desiccation of the disc. These results indicate that echinoderm tube foot discs behave like a viscoelastic material; i.e. they deform elastically under rapidly applied forces and behave viscously under slowly acting forces.

To the best of our knowledge, no other studies have been published on the material properties of adhesive surfaces from marine invertebrates. However, such studies have been made on adhesive pads of insect legs. Some insects possess smooth flexible pads whose function is to maximize contact area with the substratum, regardless of the surface micro-texture, and to secrete a lipid-like substance that is delivered to the contact area, constituting an important component of attachment (Scherge and Gorb, 2001). Like echinoderm tube foot discs, smooth insect pads demonstrate viscoelastic properties of the material. The smooth pad of the grasshopper *Tettigonia viridissima* attaches through a combination of an adhesive secretion on the pad surface and a highly deformable pad material. Gorb et al. (2000) reported that pads pressed against a structured silicon surface showed surface indentation patterns that replicated the pattern of the silicon surface. Under high loads, indentation corresponded to the height of silicon structures, and under lower loads very weak deformations occurred. The smooth pad of *T. viridissima* possesses an elastic modulus of 27.2 kPa, which is not very different from that of the echinoderm tube foot disc. Although the relaxation behaviour is different from that of the echinoderm tube foot disc, elastic moduli from both attachment systems are in the same range.

The deformability and viscoelastic properties of the grasshopper attachment pad have been related to its fibrous composite nature (Gorb et al., 2000). Indeed, the cuticle constituting the pad is made up of uniformly distributed fibres, orientated perpendicularly to the pad surface. In the vicinity of the cuticle surface, these fibres branch into numerous smaller fibres. Such an organization presumably provides flexibility at two levels: (1) the local level, when preferably branched fibres deform, and (2) the global level, when the main fibres also deform. The first level of deformation is responsible for adapting the pad surface to the substratum micro-roughness, whereas the second one can fit the pad to its macro-roughness (Gorb et al., 2000). Interestingly, the echinoderm tube foot disc is strikingly similar to the insect smooth attachment pad in its organization, though in this case the fibres are made up of collagen and manoeuvre themselves between the epidermal cells. It may be suggested that the fine collagen branches provide adaptability of the disc surface to the small irregularities of the substratum, while the main fibres or lamellae fit the disc to the macrosculpture of natural substrata.

A model for the adhesion of tube feet on rough substrata

The echinoderm tube foot disc shows both elastic and viscous behaviours under load. To enable strong attachment between the disc material and the substratum, a close proximity between opposite surfaces is required, which can be achieved through high flexibility of at least one of the materials. Echinoderms' discs proved to be highly deformable; their viscous behaviour under slow self-imposed forces enables them to replicate surface profiles, leading to an increase of the contact area between the disc and the substratum. Then, the adhesive is deposited as a film, whose thinness is advantageous for generation of strong adhesion, as shown for other glue-based systems (Kendall, 2001). Therefore, echinoderms are able to adapt to the substratum roughness by means of disc flexibility. Very small surface irregularities, in the nanometre range, can presumably be filled out with the adhesive secretion. When attached strongly to the substratum, echinoderms are also exposed to strong external forces. It can be hypothesized that, under short pulses of wave-generated forces, attached discs behave elastically, distributing the stress along the entire contact area. This would avoid crack generation and thus precludes disc peeling and tube foot detachment.

List of symbols

E, E_0, E_1	elastic moduli
F_a	adhesion force
F_c	compression force
l	thickness of the disc
L_r	profile length ratio
r	radius of the disc
R_a	mean roughness of the profile
R_z	maximum height of the profile
S	surface area
t	time
T	tenacity
T_c	corrected tenacity
Δl	deformation
τ	time of relaxation

We thank A. Peressadko and P. Postiau for technical assistance. R.S. benefited from a doctoral grant of the Foundation for Science and Technology of Portugal (SFRH/BD/4832/2001), and S.G. from a grant of the Federal Ministry of the Education, Science and Technology, Germany (project Bionik – Competition). P.F. is Research Associate of the National Fund for Scientific Research of Belgium (FNRS). This study is a contribution of the Centre Interuniversitaire de Biologie Marine (CIBIM).

References

Baier, R. E., Shafrin, E. G. and Zisman, W. A. (1968). Adhesion: Mechanisms that assist or impede it. *Science* **163**, 1360-1368.

Cheung, P. J., Ruggieri, G. D. and Nigrelli, R. F. (1977). A new method for obtaining barnacle cement in the liquid state for polymerization studies. *Mar. Biol.* **43**, 157-163.

Crisp, D. J., Walker, G., Young, G. A. and Yule, B. (1985). Adhesion and substrate choice in mussels and barnacles. *J. Colloid Interf. Sci.* **104**, 40-50.

Dougherty, W. J. (1990). SEM observations on the interfacial surface of the cement of the adult barnacle, attached to natural and synthetic adherends. *Tissue Cell* **22**, 463-470.

Flammang, P. (1996). Adhesion in echinoderms. In *Echinoderms Studies* (ed. M. Jangoux and J. M. Lawrence), pp. 1-60. Rotterdam: Balkema.

Flammang, P. (2003). The glue of sea cucumber Cuvierian tubules: a novel marine bioadhesive. In *Marine Biotechnology: An Overview Of Leading Fields* (ed. S. Colliec-Jouault, J. P. Bergé, J. Guézennec, J. Fleurence, Y. Le Gal and P. Roy), pp. 176-185. Éditions Ifremer, Actes Colloq.

Flammang, P. and Jangoux, M. (1993). Functional morphology of coronal and peristomeal podia in *Sphaerechinus granularis* (Echinodermata, Echinoida). *Zoomorphology* **113**, 47-60.

Flammang, P. and Walker, G. (1997). Measurement of the adhesion of the podia in the asteroid *Asterias rubens* (Echinodermata). *J. Mar. Biol. Assoc. UK* **77**, 1251-1254.

Flammang, P., Demeulenaere, S. and Jangoux, M. (1994). The role of podial secretions in adhesion in two species of sea stars (Echinodermata). *Biol. Bull*. **187**, 35-47.

Flammang, P., Cauwenberge, A., Alexandre, H. and Jangoux, M. (1998). A study of the temporary adhesion of the podia in the sea star *Asterias rubens* (Echinodermata, Asteroidea) through their footprints. *J. Exp. Biol*. **201**, 2383-2395.

Flammang, P., Santos, R. and Haesaerts, D. (2005). Echinoderm adhesive secretions: From experimental characterization to biotechnological applications. In *Progress in Molecular and Subcellular Biology, Marine Molecular Biotechnology, Echinodermata* (ed. V. Matranga), pp. 199-218. Berlin: Springer-Verlag.

Gabe, M. (1968). *Techniques Histologiques*. Paris: Masson.

Gorb, S., Jiao, Y. and Scherge, M. (2000). Ultrastructural architecture and mechanical properties of attachment pads in *Tettigonia viridissima* (Orthoptera Tettigoniidae). *J. Comp. Physiol*. *A* **186**, 821-831.

Grenon, J. F. and Walker, G. (1981). The tenacity of the limpet, *Patella vulgata* L. An experimental approach. *J. Exp. Mar. Biol. Ecol*. **54**, 277-308.

Kendall, K. (2001). *Molecular Adhesion and its Applications. The Sticky Universe*. New York: Kluwer Academic/Plenum Publishers.

Paine, V. L. (1926). Adhesion of the tube feet in starfishes. *J. Exp. Zool.* **45**, 361-366.

Roscoe, D. T. and Walker, G. (1995). Observations of the adhesion of the calcareous tube of *Pomatoceros lamarckii* and the holdfast of *Laminaria digitate*. *Biofouling* **9**, 39-50.

Scherge, M. and Gorb, S. (2001). *Biological Micro- And Nanotribology*. Berlin: Springer-Verlag.

Thomas, L. A. and Hermans, C. O. (1985). Adhesive interactions between the tube feet of a starfish, *Leptasterias hexactis*, and substrata. *Biol. Bull.* **169**, 675-688.

Vincent, J. (1990). *Structural Biomaterials*. Princeton: Princeton University Press.

Wainwright, S. A., Biggs, W. D., Currey, J. D. and Gosline, J. M. (1976). *Mechanical Design In Organisms*. Princeton: Princeton University Press.

Waite, J. H. (1987). Nature's underwater adhesive specialist. *Int. J. Adhes. Adhes.* **7**, 9-14.

Waite, J. H. (2002). Adhesion à la moule. *Integr. Comp. Biol.* **42**, 1172-1180.

Walker, G. (1987). Marine organisms and their adhesion. In *Synthetic Adhesives and Sealants* (ed. W. C. Wake), pp. 112-135. Chichester: John Wiley & Sons.

Whittington, I. D. and Cribb, B. W. (2001). Adhesive secretions in the Platyhelminthes. *Adv. Parasitol.* **48**, 101-224.

Young, G. A. and Crisp, D. J. (1982). Marine animals and adhesion. In *Adhesion* (ed. K. W. Allen), pp. 19-39. London: Applied Sciences.

Yule, A. B. and Walker, G. (1984). The temporary adhesion of barnacle cyprids: effects of some differing surface characteristics. *J. Mar. Biol. Assoc. UK* **64**, 429-439.

Yule, A. B. and Walker, G. (1987). Adhesion in barnacles. In *Crustacean Issues, Biology of Barnacles* (ed. A. J. Southward), pp. 389-402. Rotterdam: Balkema.